

# PROCEEDINGS OF SPIE

[SPIDigitalLibrary.org/conference-proceedings-of-spie](https://spiedigitallibrary.org/conference-proceedings-of-spie)

## Backscattered light properties during femtosecond laser ablation and development of a dynamic interferometric focusing system

Marcus Paulo Raele, Ricardo Elgul Samad, Anderson Zanardi Freitas, Lucas De Pretto, Marcello Magri Amaral, et al.

Marcus Paulo Raele, Ricardo Elgul Samad, Anderson Zanardi Freitas, Lucas De Pretto, Marcello Magri Amaral, Nilson Dias Vieira, Niklaus U. Wetter, "Backscattered light properties during femtosecond laser ablation and development of a dynamic interferometric focusing system," Proc. SPIE 10525, High-Power Laser Materials Processing: Applications, Diagnostics, and Systems VII, 105250H (15 February 2018); doi: 10.1117/12.2285899

**SPIE.**

Event: SPIE LASE, 2018, San Francisco, California, United States

# Backscattered light properties during femtosecond laser ablation and development of a dynamic interferometric focusing system

Marcus Paulo Raelé<sup>a\*</sup>, Ricardo Elgul Samad<sup>a</sup>, Anderson Zanardi Freitas<sup>a</sup>, Lucas De Pretto<sup>a</sup>, Marcello Magri Amaral<sup>b</sup>, Nilson Dias Vieira Jr<sup>a</sup> and Niklaus U Wetter<sup>a</sup>.

<sup>a</sup>Instituto de Pesquisas Energéticas e Nucleares, IPEN–CNEN/SP, Av. Prof. Lineu Prestes, 2242 – Cidade Universitária – CEP 05508-000, São Paulo – SP – Brasil

<sup>b</sup>Universidade Brasil, Biomedical Engineering, Rua Carolina Fonseca 235 – Itaquera CEP 08230-030, São Paulo – SP – Brasil

## ABSTRACT

The backscattered light originated when machining with femtosecond laser pulses can be used to accurately measure the processed surface position through an interferometer, as recently demonstrated by our group, in a setup that uses the same laser beam for ablation and inspection. The present work explores the characteristics of the laser light reflected by the target and its interaction with the resulting plasma to better understand its propagation physics and to improve the dynamic focusing system. The origin of this returning radiation was studied and has been traced, mainly, from the peripheral area of the focal spot (doughnut-like). By means of a Mach-Zehnder setup, the interferometric pattern was measured and analyzed aiming to access the influences of the plasma on the laser beam properties, and therefore on the retrieved information. Finally, the wavefront of the laser that creates and propagates through the plasma was characterized using a Shack-Hartmann sensor.

**Keywords:** Femtosecond ablation, low coherence, interferometry, backscattered light.

## 1. INTRODUCTION

The unique properties of ultrafast femtosecond (fs) laser pulses and their interaction with matter[1] allowed machining of a new range of materials and on a new size scale. Due to the high peak power and the absence (or negligible) thermal effects when using near-IR femtosecond pulses for ablation, micrometer sized structures can be produced in materials that strongly interact with the laser wavelength or not, like metals and glass, respectively.

In order to achieve such machining precision, focusing is crucial for getting a small beam waist ( $2w_0$ ), Figure 1 left, for lateral resolution and to have a short confocal parameter for high axial resolution. The two can be obtained with high numerical aperture (NA) focusing optics. This approach covers the machining of extremely flat surfaces, where after the overlapping the surface with the confocal length, the CNC can take control and mill the substrate.

However, irregular profiles, whose topography are not previously known and, therefore cannot be corrected, can compromise the advantages provided by the fs laser machining, diminishing the potential applications of this tool. Focusing correction systems are available; however, most of them are based on capacitive sensors that cannot cope with dielectric samples such as ceramics, polymers and glasses.

Our group approached this issue analyzing, in real time, the low coherence interferometric patterns of a Michelson like setup [2], Figure 1 right, that was able to constantly monitor the sample's surface position by analyzing the reflected portion of light by the sample surface when machining. Knowing the position of the focal plane from previous calibration, the system is capable of moving the sample axially to keep the surface within the confocal parameter during almost every point of the engraving path, even in samples with strongly irregular or unknown profiles.

---

\* [mpraele@ipen.br](mailto:mpraele@ipen.br)

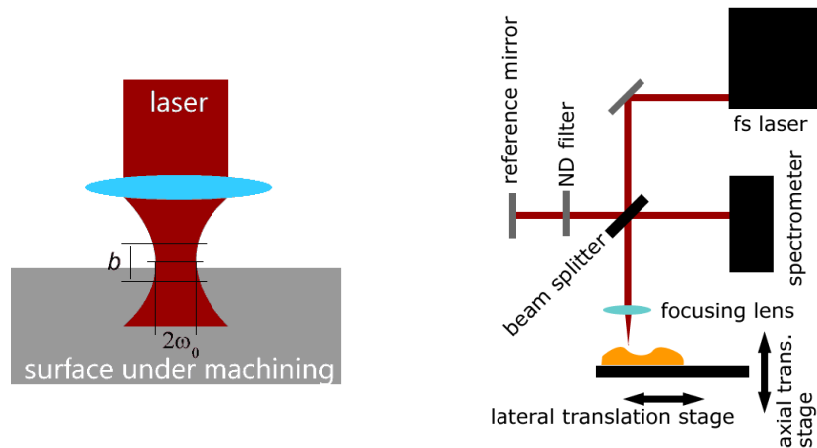


Figure 1: Left: the overlap between the sample and the confocal zone ( $b$ ) and the representation of the beam waist ( $2w_0$ ). Right: experimental setup for a dynamic focusing system based on low coherence interferometry. Both illustrations were extracted from Raelle et al[2].

This system proved to be effective and viable. However, three questions were left open about the properties of the reflected light by the sample:

### 1.1 Where exactly does the reflected light come from in the laser-sample interaction region?

The focusing evaluation by low coherence interferometry (LCI) is based on the measurement of the optical path difference between the interferometer's arms (reference arm and sample arm) using the reflected light by the two. The reference arm does have a mirror, and therefore the position (optical path) and the reflectivity is easily controlled and known. On the other hand, the optical interaction happening on the sample is more complex. Once that the sample starts to be ablated, the surface presents an "erosion" that increases as the laser pulses hit the target's surface. During this process, a laser fraction will be reflected. At the same time, part of the laser has not enough intensity to eject material, and will be absorbed as heat and also partially reflected. In this way is important to determine where the useful signal is originated, Figure 2.

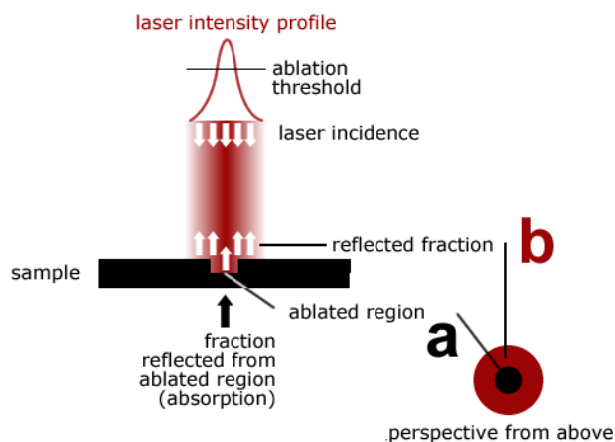


Figure 2: Illustration of the laser beam interaction with the sample and two possible regions that provides useful light reflection to form the interferometric signal.

### 1.2 How does the plasma alter the laser which passes through it?

During the laser ablation process, the laser pulse creates a plasma plume through which the laser pulse passes. At high repetition rates, there might be even some reflection from the plasma created by the previous pulse. It is known that plasma under the right conditions, can strongly interact with the incident laser [3], however, it is not known how the plasma modifies the interferometric pattern on a LCI system.

### 1.3 How does the plasma alter the laser wavefront of the passing laser?

Another interesting feature of lasers beams are the wavefront characteristics. It is important from the focusing point of view and also from the interferometric point of view (for time domain LCI systems[4]).The plasma has different densities across its profile altering differently the beam core and borders.

## 2. MATERIALS, METHODS AND RESULTS

For the following experiments a pulsed femtosecond laser system was used. This system is a Ti:Sapphire CPA laser (Femtopower Compact Pro CE-Phase HP/HR from Femtolasers), continuously generating 25 fs (FWHM) pulses centered at 775 nm with 40 nm of bandwidth (FWHM), at a maximum repetition rate of 4 kHz, with up to 800  $\mu$ J of pulse energy. For detection a spectrometer (OceanOptics USB 4000, spectral range 599-898 nm) coupled to a monomode optical fiber with a hybrid connectorization FC/PC-SMA and collimation optics (Thorlabs model F240FC-850).

### 2.1 Backscattering region

In order to determine the region where the reflected laser fraction comes from, an experimental setup was designed in which a thin metal foil was placed at the laser focus and a power meter was positioned behind it connected to the acquisition system, Figure 3. When the laser was enabled, the ablation process would take place and eventually get through the sample.

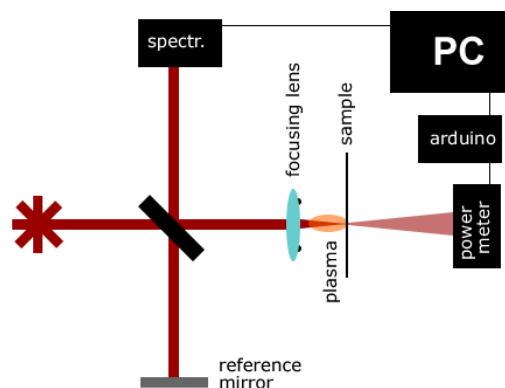


Figure 3: Experimental setup.

The results of this evaluation are shown in Figure 4, where the optical scattering profile was acquired as a function of time along with the energy of the laser that passes through the hole produced in the metal foil. Once the laser shutter was opened (pointed by the vertical red line), the surface of the sample was located by the interferometer at  $\sim 250 \mu\text{m}$  after approximately 400 ms from the beginning of the data recording. The power meter accuses the metallic foil of being drilled almost instantaneously with the release of the beam, the transmitted power grows expressively until the highest backscattering intensity value was recorded at 250  $\mu\text{m}$  (magenta line) with a 241 ms from the shutter opening, with the value of  $\sim 150$  a.u., the value then stabilizes at  $\sim 100$  a.u., indicating that the ablation process ceased.

From this first analysis we conclude that the signal used for ablation monitoring originates in two regions, according to Figure 2, region "a" and region "b" with 30% and 70%, respectively (for the metal sample).

Also in Figure 4, the red, green and black hachured areas project the average of the scattering profile in the right at three moments: without the laser, during ablation process and after the perforation of the sample, respectively. Significant noise is noted in the signal during the ablation occasioned or by saturation of the signal, or as a result of the plasma

emissions. The energy incident on the sample was 19.2  $\mu\text{J}$ , of which 7.7  $\mu\text{J}$  were transferred to the detector after the hole was etched.

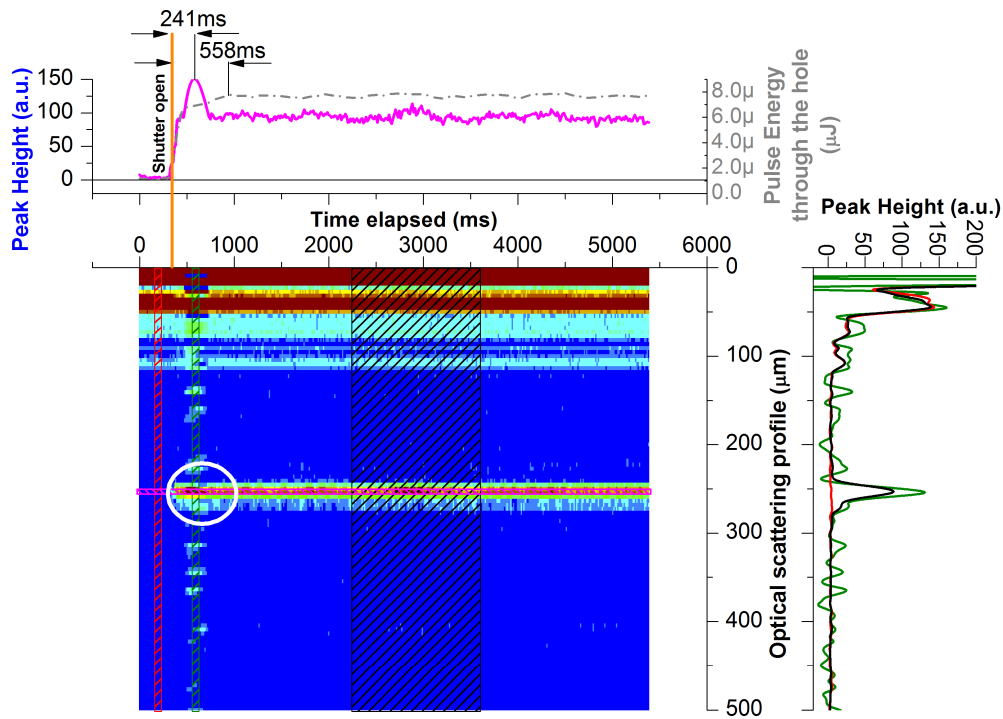


Figure 4: Optical scattering profile vs. elapsed time.

Furthermore, when looking closely, at the circled region in the Figure 4, it is possible to see that the system returned also information about the crater time evolution during the ablation process. In Figure 5, a structure that appears below the foil surface indicates that the material is being removed (white arrow).

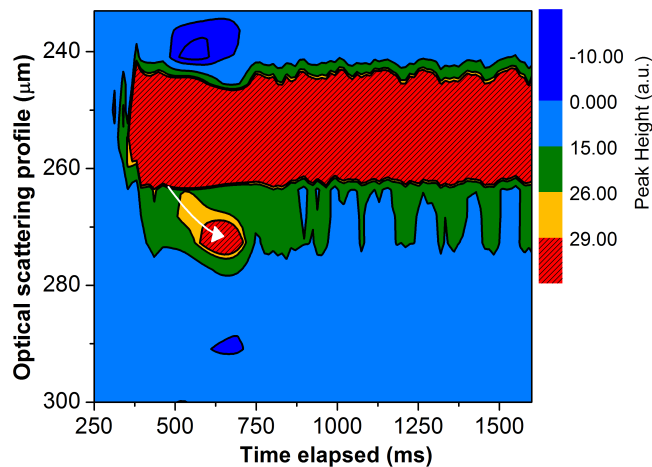


Figure 5: A closer look at the circled region on Figure 4. The structure below the surface indicates the ablation process and the crater evolution, i.e., was formed and light scattering structure below the very surface of the foil, the total signal is an mixture of light coming from regions “a” and “b” from Figure 2.

## 2.2 Plasma and low coherence interferometry.

To inspect how the plasma can disturb the reflected signal by the sample under ablation, a slightly different setup was mounted based on a Mach-Zehnder configuration that helps to avoid unwanted and uncontrollable effects inherent to solids ablation, such as crater formation, sample parallelism, translation velocity variations, etc. In this setup, any change in the laser properties can only be caused by the plasma itself. The procedure used to avoid modification of the laser system was to use absorptive neutral density filters (NDF) in the setup entrance and in the detector collimation entrance, positions “NDF 1” and “NDF 2” at Figure 6. Using a set of 3 NDF (0.4, 0.3 and 0.2) it was possible to increase the power in the interferometer without increasing the laser power on the detection system. The focusing and collimation lenses had 1 inch of effective focusing length and 1 inch in diameter, and the compensator was used to set the desired optical path difference between both arms (the arm with lenses had 527.33  $\mu\text{m}$  more optical path than the reference arm). The spectral interferogram was then processed[5] to return the optical path difference in real time.

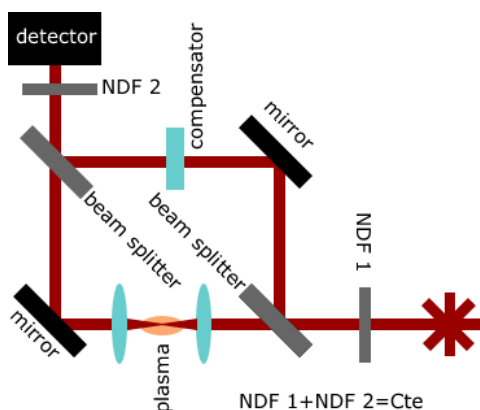


Figure 6: Mach-Zehnder low coherence interferometer.

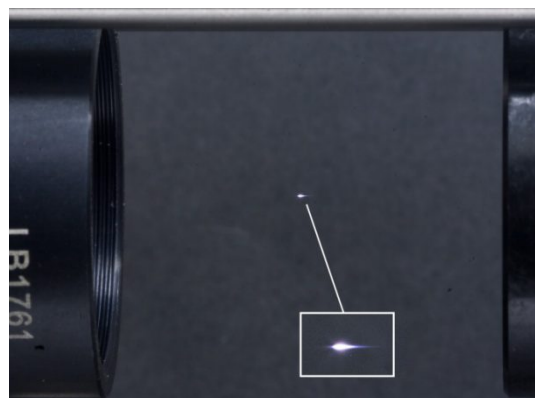


Figure 7: Plasma aspect. The laser incidence comes from the right.

Figure 8 shows the spectra from the lensed arm and the spectra of the combined contribution of both arms (interferogram). Taking as baseline the spectrum at the lowest energy, where there is no plasma formation, it is noticeable that the laser beam that is focused and collimated suffers nonlinear effects such as spectral broadening and absorption as the energy grows, deforming the spectrum that will interfere with the reference one. The broadening process present characteristics of self/cross-phase modulation[6, 7] prominent in energies above 80  $\mu\text{J}$  (rippled structure below 750 nm). Nonetheless the interferogram is formed clearly independent of the pulse energy, despites at 120  $\mu\text{J}$ . Figure 7 shows a photograph of the plasma formed at the maximum laser energy.

After processing the interferometric pattern [4] (basically through a Fourier Transform), the optical path difference between both arms can be calculated as shown in Figure. As the pulse energy grows, the peaks decrease in amplitude and are displaced to smaller optical path differences. The peak decreasing can be understood by the modification on the spectrum of the plasma arm, which can no longer interfere completely with the reference spectrum. The modification of the peak position, however, indicated that the plasma arm was “shrinking” by a few microns as the laser energy increases.

This effect can be explained if the electron density in the plasma is smaller than the critical electron density (when the plasma frequency and the laser frequency are equal), situation in which the refractive index can be smaller than unity[8]. This behavior occurred in a very linear way with laser energy, as shown at Figure 10, except for the maximum energy which degenerated the signal strongly, making the Gaussian fit unfeasible due to another formation in the same region. The peak width (coherence length), shown in Figure 11, remained stable until the optical breakdown regime established itself, which also made it difficult the fitting process.

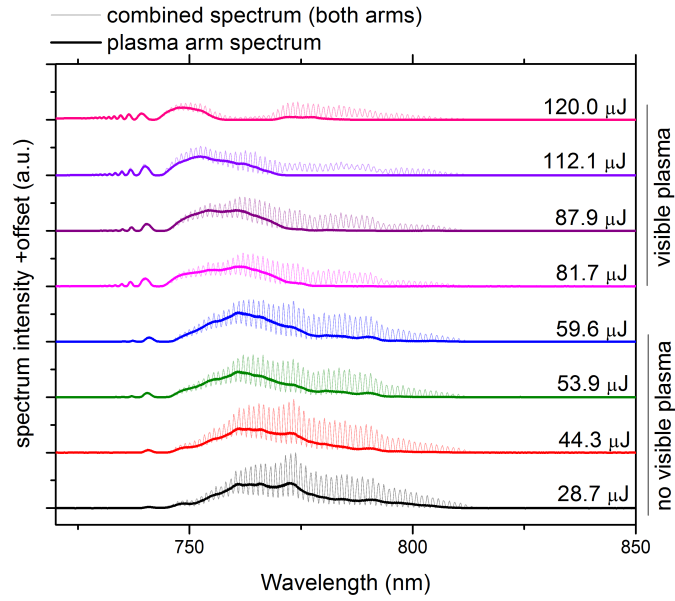


Figure 8: Spectra of function of pulse energy. The stronger lines are related to the focusing arm only spectra. The lighter lines are the spectral interferograms resulting from the contributions of both arms.

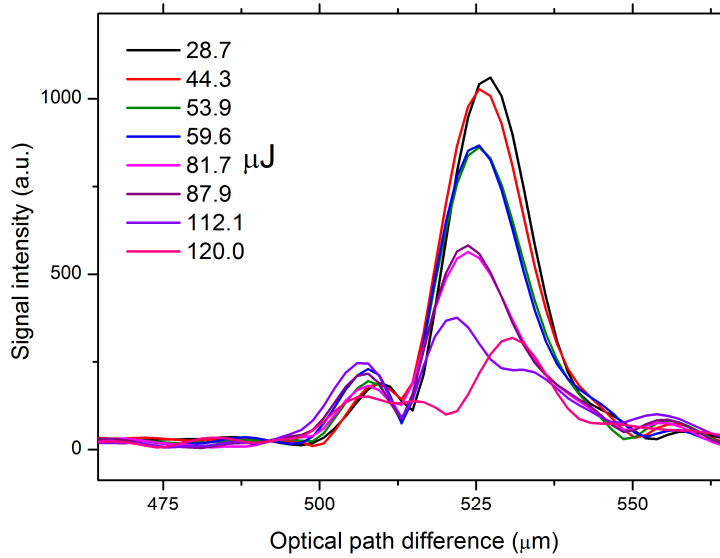


Figure 9: Optical path difference between both arms as a function of pulse energy extracted from the spectral interferograms from Figure 8.

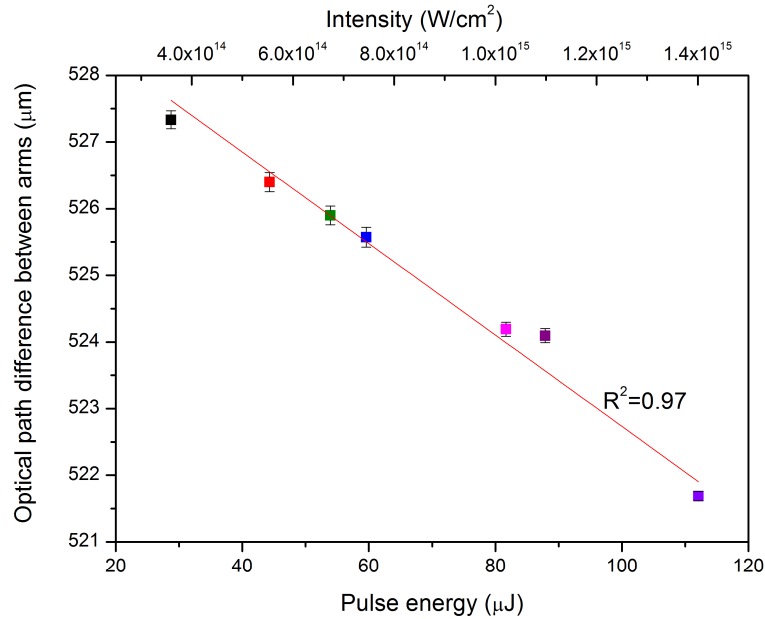


Figure 10: Peak centroids (extracted from Gaussian fits) as a function of the pulse energy. The 120 $\mu$ J pulse could not be fitted properly, therefore is not presented.

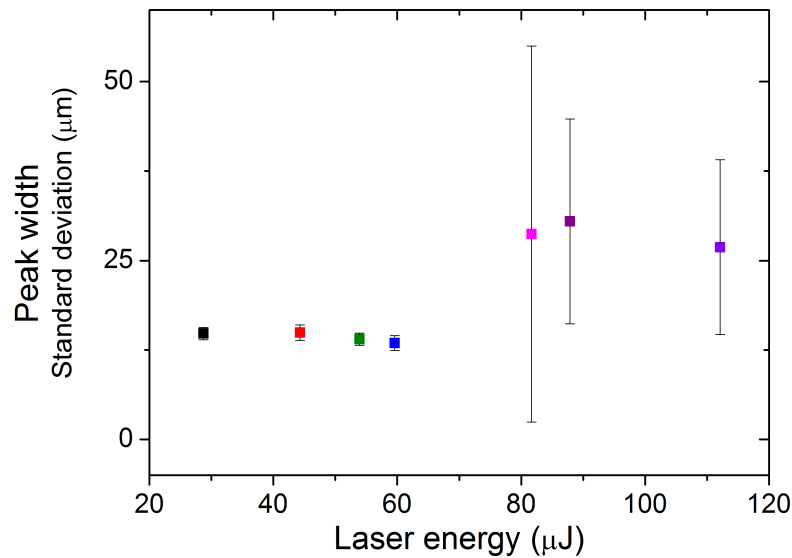


Figure 11: Peak width extracted from Gaussian fits from Figure 9, the values are related to the standard deviation.

### 2.3 Wavefront

A Shack-Hartmann Wavefront Sensor (ThorlabsWFS150-5C) was positioned after plasma formation, as shown in Figure 12. The procedure was started with the NDF placed at “NDF 1” (Figure 12), configuration that not allowed to plasma formation, and then sensor’s software was then was set to interpret the wavefront as a plane wave, as calibration measurement (grey wireframe at Figure 13). Then the NDF was moved to “NDF 2” which allowed enough pulse energy to create plasma in the focal region, then a new measurement was performed resulting in the black wireframe at Figure



13, which shows that the beam peripheral area was delayed, while the very center of the beam has advanced to values smaller than zero, corroborating the results presented at Figure 10.

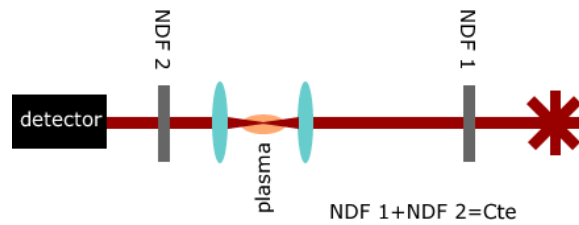


Figure 12: Experimental setup for wavefront characterization.

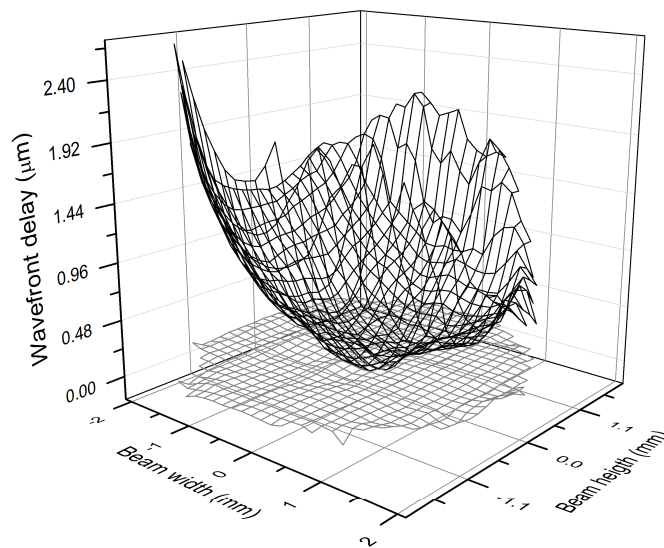


Figure 13: The grey wireframe represents the laser without energy enough to open creates plasma, and it was used to calibrate the Shack-Hartmann sensor. The black wireframe shows the laser wavefront when plasma is present.

### 3. CONCLUSIONS

The aim of this study was to better understand the processes that can hamper the proper formation of an interferometric low coherence signal aiming the development of an auto focusing system based on the laser reflection by the material under machining. Firstly, the origin of the reflected signal was traced to the peripheral area of the focused beam, where it doesn't reach the ablation threshold; nonetheless, a small contribution from the center area is present and can even be used to monitor the ablation process.

The plasma plays an important role on the deterioration of the interferometric signal due the spectral broadening and shielding, it also, due to refractive index properties, that can lead to system errors when evaluating the optical path difference between the interferometer's arms.

Finally, the wavefront was also considerably modified by the plasma, which could pose problems to time domain low coherence interferometry systems[4], which analyses directly the pulse cross correlation, considering that the plasma is

stretching the pulse duration. More concerning though, is the implications on the spot size considering high resolution machining.

## ACKNOWLEDGEMENT

We thank the grants #2015/24878-0 and 13/26113-6 from the São Paulo Research Foundation (FAPESP) , 573916/2008-0 from National Research Council (CNPq) and The National Council for Scientific and Technological Development (CNPq/INCT) – Brazil (grant #465763/2014-6).

## REFERENCES

- [1] R. E. Samad, L. M. Machado, N. D. Vieira Junior *et al.*, [Ultrashort Laser Pulses Machining] InTech, (2012).
- [2] M. P. Raelle, L. R. De Pretto, R. E. Samad *et al.*, "Development of a dynamic interferometric focusing system for femtosecond laser machining," Proceedings of SPIE. 10094(2017).
- [3] C. H. Fan, J. Sun, and J. P. Longtin, "Plasma absorption of femtosecond laser pulses in dielectrics," Journal of Heat Transfer-Transactions of the Asme, 124(2), 275-283 (2002).
- [4] A. Z. Freitas, M. M. Amaral, and M. P. Raelle, [Optical Coherence Tomography: Development and Applications] InTech, Rijeka, 20 (2010).
- [5] M. E. Brezinski, [Optical Coherence Tomography: Principles and Applications] Elsevier Science, (2006).
- [6] L. L. Yu, Y. Zhao, L. J. Qian *et al.*, "Plasma optical modulators for intense lasers," Nature Communications, 7, (2016).
- [7] S. P. Le Blanc, [Plasma-induced self-phase and cross-phase modulation of femtosecond laser pulses] RICE, Houston, Texas(1994).
- [8] J. Hermann, S. Bruneau, and M. Sentis, "Spectroscopic analysis of femtosecond laser-induced gas breakdown," Thin Solid Films, 453, 377-382 (2004).